Atmospheric Environment 70 (2013) 98–107

Contents lists available at SciVerse ScienceDirect

Atmospheric Environment

journal homepage: www.elsevier.com/locate/atmosenv

Dispersion and photochemical evolution of reactive pollutants in street canyons

Kyung-Hwan Kwak, Jong-Jin Baik*, Kwang-Yeon Lee

School of Earth and Environmental Sciences, Seoul National University, Seoul 151-742, Republic of Korea

HIGHLIGHTS

- Dispersion and photochemical evolution of reactive pollutants in street canyons.
- Photochemical ages of NO_x and VOC as a function of concentration ratios.
- Favorable O_3 chemical production in a more aged air mass.
- Sensitivities to NO_x and VOC emission rates, photolysis rate, and ambient wind speed.
- A diagram capturing the relative importance between O_3 and OH oxidation processes.

ARTICLE INFO

Article history:
Received 13 September 2012
Received in revised form
27 December 2012
Accepted 3 January 2013

Keywords:
Street canyon
Dispersion
CFD model
CBM–IV
Photochemical age
Oxidation process

ABSTRACT

Dispersion and photochemical evolution of reactive pollutants in street canyons with canyon aspect ratios of 1 and 2 are investigated using a computational fluid dynamics (CFD) model coupled with the carbon bond mechanism IV (CBM–IV). Photochemical ages of NO_x and VOC are expressed as a function of the NO_2-to-NO_x and toluene-to-xylene ratios, respectively. These are found to be useful for analyzing the O_3 and OH oxidation processes in the street canyons. The OH oxidation process (O_3 oxidation process) is more pronounced in the upper (lower) region of the street canyon with a canyon aspect ratio of 2, which is characterized by more (less) aged air. In the upper region of the street canyon, O_3 is chemically produced as well as transported downward across the roof level, whereas O_3 is chemically reduced in the lower region of the street canyon. The O_3 chemical production is generally favorable when the normalized photochemical ages of NO_x and VOC are larger than 0.55 and 0.28, respectively. The sensitivities of O_3 chemical characteristics to NO_x and VOC emission rates, photolysis rate, and ambient wind speed are examined for the lower and upper regions of the street canyon with a canyon aspect ratio of 2. The O_3 concentration and the O_3 chemical production rate divided by the O_3 concentration increase as the NO_x emission rate decreases and the VOC emission rate and photolysis rate increase. The O_3 concentration is less sensitive to the ambient wind speed than to other factors considered. The relative importance of the OH oxidation process compared to the O_3 oxidation process increases with increasing NO_x emission rate and photolysis rate and decreasing VOC emission rate. In this study, both O_3 and OH oxidation processes are found to be important in street-canyon scale chemistry. The methodology of estimating the photochemical ages can potentially be adopted to neighborhood scale chemistry.

1. Introduction

In urban areas, pollutants are emitted from various types of sources and they are then transformed and transported in the atmosphere. A freshly emitted air mass mixes with the background air, and primary pollutants in the air mass are oxidized by hydroxyl radical (OH), hydroperoxy radical (HO_2), organic peroxy radicals (RO_2), and ozone (O_3). Mixing and photochemical processes interacting with each other change the characteristics of an air mass.

Flow in an urban street canyon is largely isolated from flow in the overlying atmosphere and pollutants from vehicles are emitted directly into the street canyon, thus exhibiting the distinct characteristics of an air mass. In a street canyon, the time scale of the photochemical evolution of an air mass is short and the length scale of the pollutant dispersion is small. Computational fluid dynamics (CFD) models have been used to examine the photochemical evolution of air masses in street canyons. Using CFD models that include simple photochemical reactions, Baker et al. (2004) and

* Corresponding author. Tel.: +82 2 880 6990; fax: +82 2 883 4972.
E-mail address: jjbaik@snu.ac.kr (J.-J. Baik).

1352-2310/$ – see front matter © 2013 Elsevier Ltd. All rights reserved.
http://dx.doi.org/10.1016/j.atmosenv.2013.01.010

Baik et al. (2007) showed that the O_3 concentration is lower in a street canyon than above it because O_3 is largely depleted by the emitted NO. Baik et al. (2007) performed the budget analysis of the O_3 concentration and showed that the magnitude of the chemical reaction term is comparable to that of the advection or turbulent diffusion term. Using the field Monte Carlo method, Garmory et al. (2009) emphasized that the variances of some radical species in the carbon bond mechanism IV (CBM–IV) are significant near the rooftop level where the mixing process is active. These previous studies showed only the importance of O_3 oxidation in determining the dispersion of NO, NO_2, and O_3. Recently, Kwak and Baik (2012) developed a CFD model coupled with the CBM–IV. They found that the role of OH oxidation in the dispersion of reactive pollutants in a street canyon is crucial. Kim et al. (2012) also insisted that the OH oxidation of volatile organic compound (VOC) needs to be included in street-canyon scale chemistry. These two recent studies imply that the photochemical evolution of pollutants in a street canyon is significantly affected by the OH oxidation process as well as the O_3 oxidation process.

Many observational studies have been undertaken to investigate the photochemical evolution of air masses in urban areas. Several VOC concentration ratios have been used to estimate the evolution of air masses regarding photochemical processes (Calvert, 1976; Roberts et al., 1984; McKeen et al., 1996). A photochemical age, defined as the time-integrated exposure of an air mass to OH radical from the point of emission to the point at which observations are made, is based on the different reactivities of VOCs to OH (Kleinman et al., 2003). For example, de Gouw et al. (2005) and Apel et al. (2010) used the ratio between observed toluene (as a non-photochemically produced species) and observed benzene (as a long-lived species) following Roberts et al. (1984) and showed that more photochemically aged plumes have smaller toluene-to-benzene ratios in New England and in the outflow of the Mexico City metropolitan area, respectively. Despite its usefulness, the photochemical age has weaknesses resulting from certain assumptions. The photochemical age is valid under the assumptions on emission of VOCs from a single source location, reaction of VOCs only with OH radical, non-diffusive transport of VOCs, and clean background air with negligible VOC concentrations (Rudolph and Johnen, 1990; Kleinman et al., 2003).

A street canyon is a space in which the above assumptions are satisfactorily met. Thus, the photochemical age can be employed. In addition to the previously suggested OH oxidation process, the O_3 oxidation process needs to be included in the photochemical age in a street canyon. In this study, we express the photochemical age of NO_x (= NO + NO_2) as a function of the NO_2-to-NO_x ratio (NO_2/NO_x) representing the O_3 oxidation process and the photochemical age of VOC as a function of the toluene-to-xylene ratio (TOL/XYL) representing the OH oxidation process. Using these photochemical ages based on the concentration ratios, the O_3 and OH oxidation processes in a street canyon are examined. This is the first objective of the present study.

A street canyon with a canyon aspect ratio of 1 is typically considered to examine flow and dispersion in a street canyon. In fact, large amounts of pollutants emitted from the bottom of a street canyon with a canyon aspect ratio of 1 are ventilated directly through the roof level. Baik and Kim (1999) and Li et al. (2009) revealed that multiple vortices appear in street canyons with larger canyon aspect ratios. In a street canyon with a canyon aspect ratio of 2, two counter-rotating vortices appear and they act to suppress the upward transport of emitted pollutants, resulting in a small vertical pollutant flux at the roof level (Baik and Kim, 2002). Therefore, a street canyon with a canyon aspect ratio of 2 is a suitable choice to examine the photochemical evolution of an air mass and its related processes therein. Many factors such as NO_x and VOC emission rates, photolysis rate, and ambient wind speed can affect transport and chemical production of reactive pollutants in a street canyon. The second objective of this study is to examine O_3 chemical characteristics that are sensitive to these factors in the lower and upper regions of the street canyon.

2. Methods

2.1. Photochemical age

An air mass is aged over time through mixing with the background air and through photochemical reactions. Because of the different reactivities of chemical species, the concentrations of chemical species decrease at different rates in an air mass. Concentration ratios have been traditionally applied to studies in urban areas (Calvert, 1976) and rural areas (Roberts et al., 1984) to estimate unknown OH concentrations or the diluting effect of an air mass. In some previous studies, the concentration ratios were proposed as a photochemical aging indicator (Nelson and Quigley, 1983; Roberts et al., 1984).

To apply a photochemical age to street-canyon scale chemistry, we use two different concentration ratios, NO_2/NO_x and TOL/XYL.

$$NO + O_3 \rightarrow NO_2 + O_2, \quad \text{(R1)}$$

$$NO_2 \rightarrow NO + O, \quad \text{(R2)}$$

$$TOL + OH \rightarrow \text{products}, \quad \text{(R3)}$$

$$XYL + OH \rightarrow \text{products}. \quad \text{(R4)}$$

NO_2/NO_x is an indicator of O_3 oxidation of NO to NO_2. NO_2 is produced by the NO titration of O_3, as shown in (R1). As an air mass ages, NO_2/NO_x increases until the NO_2 production is balanced by the NO_2 loss shown in (R2). The O_3 oxidation of NO to NO_2 is more pronounced in street-canyon scale chemistry, whereas the OH oxidation of NO_x to NO_y (total reactive nitrogen) is more pronounced in regional scale chemistry. TOL/XYL is an indicator of OH oxidation of VOCs. Because TOL is less reactive than XYL with OH [see (R3) and (R4)], the TOL concentration slowly decreases over time in comparison to the XYL concentration. Therefore, TOL/XYL increases as an air mass ages. It is noteworthy that TOL and XYL are more reactive than alkanes, alkenes, and benzene, which were previously used in regional scale studies on the photochemical age. As a result, TOL/XYL is an appropriate indicator for application in street-canyon scale chemistry.

The photochemical ages of NO_x (t_{NO_x}) and VOC (t_{VOC}) are expressed as a function of NO_2/NO_x and TOL/XYL, respectively. Following Parrish et al. (2007), the photochemical ages can be derived as

$$t_{NO_x} = -\frac{1}{\langle k_{NO+O_3}\rangle\langle[O_3]\rangle}\left\{\ln\left(1-\frac{[NO_2]}{[NO_x]}\right)-\ln\left(1-\frac{[NO_2]_e}{[NO_x]_e}\right)\right\}, \quad (1)$$

$$t_{VOC} = \frac{1}{\langle k_{XYL+OH}-k_{TOL+OH}\rangle\langle[OH]\rangle}\left\{\ln\left(\frac{[TOL]}{[XYL]}\right)-\ln\left(\frac{[TOL]_e}{[XYL]_e}\right)\right\}. \quad (2)$$

Here, k_{NO+O_3}, k_{XYL+OH}, and k_{TOL+OH} are the reaction coefficients between NO and O_3, XYL and OH, and TOL and OH, respectively. $\langle\rangle$ denotes the time average from the point of emission to the point at which observations are made. $[NO_2]_e$, $[NO_x]_e$, $[TOL]_e$, and $[XYL]_e$ are the concentrations of NO_2, NO_x, TOL, and XYL at the point of emission, respectively.

Then, the ratio between two normalized photochemical ages (R_{PA}) is calculated as follows.

$$R_{PA} = \frac{t_{NO_x}}{t_{NO_x}^{bg}} \Big/ \frac{t_{VOC}}{t_{VOC}^{bg}}, \quad (3)$$

where $t_{NO_x}^{bg}$ and t_{VOC}^{bg} are the background photochemical ages of NO_x and VOC, respectively. The photochemical ages normalized by their background ages, $t_{NO_x}/t_{NO_x}^{bg}$ and t_{VOC}/t_{VOC}^{bg}, simply indicate the cumulative progress of O_3 and OH oxidation processes, respectively, from the point of emission to the point of interest. If a normalized photochemical age is 0, the air has emission characteristics. If a normalized photochemical age is 1, the air has background characteristics. The normalization of photochemical age removes the uncertainty from estimating the average concentrations of O_3 and OH individually, as we simply need to estimate the concentration ratios of O_3 and OH between the street canyon and the background. If the concentration ratios of O_3 and OH are regarded as constant values, the normalized photochemical ages are still a function of NO_2/NO_x and TOL/XYL, respectively. R_{PA} indicates a progress ratio of the O_3 oxidation process to the OH oxidation process. If R_{PA} is larger than 1, the O_3 oxidation process is cumulatively faster than the OH oxidation process, while an air mass travels from the point of emission to the point of interest. On the other hand, if R_{PA} is smaller than 1, the OH oxidation process is cumulatively faster than the O_3 oxidation process. Furthermore, by taking the ratio between two normalized photochemical ages (R_{PA}), the uncertainties in the concentration ratios of O_3 and OH estimated as constants can be excluded because NO_x and VOCs share the same source and trajectory in a street canyon. $t_{NO_x}/t_{NO_x}^{bg}$, t_{VOC}/t_{VOC}^{bg}, and R_{PA} are useful for evaluating both O_3 and OH oxidation processes that are comparably important in photochemical evolution of an air mass in a street canyon.

2.2. CFD model

The CFD model used in this study is a Reynolds-averaged Navier–Stokes equations (RANS) model coupled with the CBM–IV (Kwak and Baik, 2012). The governing equations are the momentum equation, the mass continuity equation, the transport equation of reactive species, and the equations of turbulent kinetic energy and its dissipation rate. The CBM–IV has 36 reactive species and 93 reactions (Gery et al., 1989). The chemical solver is the Eulerian backward iteration (EBI) method (Hertel et al., 1993), which integrates the stiff system of photochemical reactions.

Model validation for various reactive pollutant concentrations in a deep street canyon against field or wind tunnel measurements is not possible owing to the lack of measurements. However, the CFD model was validated for horizontal velocity against wind tunnel measurements in a street canyon with street bottom heating (Baik et al., 2007). Furthermore, Kwak and Baik (2012) validated the model using the roadway measurement data (NO_2 and NO_x concentrations) following Wang et al. (2011). The validation results show the accuracy of the CFD model.

3. Experimental setup

Fig. 1 depicts the computational domain and street canyon configuration. The street canyon width (W) is 20 m, and the building height (H) considered is 20 m and 40 m. Thus, the street canyon aspect ratio (H/W) considered is 1 and 2. The domain size is 40 m × 60.1 m for $H/W = 1$ and 40 m × 100 m for $H/W = 2$. The grid interval in the x-direction is 0.5 m, and the grid interval in the z-direction is 0.5 m up to $z = 32$ m for $H/W = 1$ and $z = 68.5$ m for $H/W = 2$. Above these heights, an expansion ratio of 1.1 is applied to the grid interval in the z-direction. The ambient wind blows in the positive x-direction, and the ambient wind speed is vertically uniform at the inflow boundary. Turbulent kinetic energy and its dissipation rate at the inflow boundary are also vertically uniform based on the ambient wind speed. The air temperature is set to be 298 K (isothermal condition). For concentrations of reactive species, cyclic boundary conditions are applied at the inflow and outflow boundaries. Initial concentrations of reactive species (e.g., 10 ppb for NO and 30 ppb for NO_2 and O_3) are uniform over the computational domain. Nine emission species (NO, NO_2, and 7 VOCs) are emitted at the lowest model level ($z = 0.25$ m) in the street canyons. The 7 VOCs are FORM (formaldehyde), ALD_2 (high molecular weight aldehydes), PAR (paraffin carbon bond), OLE (olefin carbon bond), ETH (ethene), TOL, and XYL. The relative portion between NO and NO_2 emission rates is 9:1. The relative portions of the emission rates of the 7 VOCs are 56.3% for PAR, 12.4% for TOL, 11.9% for XYL, 9.5% for ETH, 6.7% for OLE, 2.1% for ALD_2, and 1.1% for FORM (Bossioli et al., 2002; Kwak and Baik, 2012). The relative portion between NO and NO_2 emission rates and the relative portions of the emission rates of the 7 VOCs are kept constant in all experimental cases.

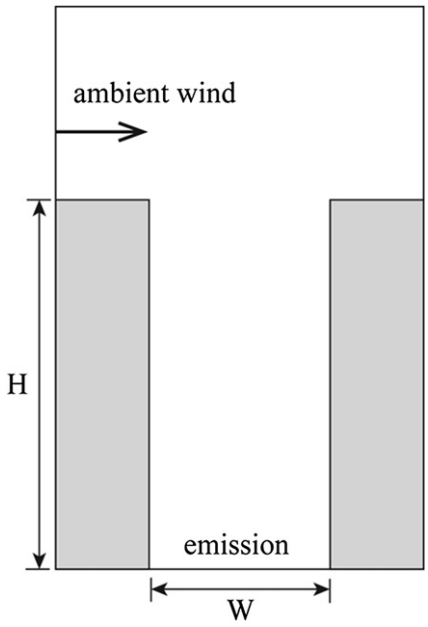

Fig. 1. Computational domain and street canyon configuration. H is the building height and W is the street canyon width.

An experiment is performed for $H/W = 1$. Fifteen experiments for $H/W = 2$ are performed to examine sensitivities to NO_x and VOC emission rates, photolysis rate, and ambient wind speed. A case with NO_x and VOC emission rates of 2 ppb s^{-1} per grid cell, no reduction in photolysis rate, and an ambient wind speed of 5 m s^{-1} is selected as the control experiment for $H/W = 2$. The sixteen different experimental cases are summarized in Table 1. In addition to the fifteen experiments for $H/W = 2$, one additional experiment that is the same as the control experiment but with the chemistry-off is performed. The CFD model is integrated for 120 min with both CFD and chemical time steps of 0.1 s. The chemical time step is set to be a half of the previous one repeatedly when the concentration does not satisfy its convergence condition in the EBI method. Emission and chemical processes are off for the first 30 and 60 min, respectively. Because concentrations of reactive species do not exactly satisfy a steady state, all results are averaged from $t = 90$ to 120 min for analysis.

Table 1
Experimental cases with different canyon aspect ratios (H/W), NO_x emission rates, VOC emission rates, J-value coefficients, and ambient wind speeds.

No.	H/W	NO_x emission rate (ppb s^{-1})	VOC emission rate (ppb s^{-1})	J-value coefficient	Ambient wind speed (m s^{-1})
1	1	2	2	1.0	5
2 (control)	2	2	2	1.0	5
3	2	1	2	1.0	5
4	2	4	2	1.0	5
5	2	6	2	1.0	5
6	2	2	1	1.0	5
7	2	2	4	1.0	5
8	2	2	6	1.0	5
9	2	2	2	0.2	5
10	2	2	2	0.4	5
11	2	2	2	0.6	5
12	2	2	2	0.8	5
13	2	2	2	1.0	3
14	2	2	2	1.0	4
15	2	2	2	1.0	6
16	2	2	2	1.0	7

4. Results and discussion

4.1. Control experiment

Many previous CFD modeling studies have shown that in street canyons O_3 is markedly depleted by NO (Baker et al., 2004; Baik et al., 2007; Garmory et al., 2009; Kwak and Baik, 2012). Kwak and Baik (2012) examined the O_3 sensitivity to precursors and concluded that the street canyon with an aspect ratio of 1 is a negatively NO_x-sensitive regime because of freshly emitted NO from mobile sources. However, it is not clear whether O_3 is always chemically reduced due to the NO titration of O_3 in a street canyon or not. In the first part of this study, we focus on O_3 chemical production and reduction in street canyons.

Fig. 2 shows the streamline and O_3 concentration fields in the $H/W = 1$ and 2 street canyons. In the $H/W = 1$ street canyon, a primary vortex and secondary corner vortices appear. In association with the primary vortex circulation, the O_3 concentration is lower than 20 ppb near the street bottom and the upwind building wall. In the $H/W = 2$ street canyon, two counter-rotating vortices, that is, a clockwise-rotating upper vortex and a counterclockwise-rotating lower vortex appear. In association with these vortices circulation, the O_3 concentration is lower than 20 ppb near the street bottom and the lower part of the downwind building wall. In the upper region of the street canyon, the O_3 concentration is generally higher than the initial O_3 concentration (30 ppb). An air mass in the lower region of the street canyon is directly affected by emission, which is similar to that in the $H/W = 1$ street canyon. On the other hand, an air mass in the upper region of the street canyon is largely affected by the background air across the roof level. In addition, air masses in the lower and upper regions of the street canyon are likely to be isolated from each other due to the counter-rotating vortices circulation. As a result, the O_3 chemical characteristics in the lower region of the street canyon can be different from those in the upper region of the street canyon.

Fig. 3 shows the fields of O_3 transport (advection plus turbulent diffusion in this study) rate and O_3 chemical production rate, which are divided by O_3 concentration, and the field of the photo-stationary state ($= [NO][O_3]/[NO_2]$). When the chemical equilibrium among NO, NO_2, and O_3 is satisfied, the photo-stationary state is equivalent to J_{NO_2}/k_{NO+O_3}. The chemical instability is large near the street bottom and the mid-level of the downwind building wall. In these two regions, O_3 is reduced chemically but is produced at almost equal rates owing to transport. Near the street bottom, O_3 is depleted by freshly emitted NO. The O_3 transport following the lower vortex compensates for this O_3 depletion. Near the mid-level of the downwind building wall, NO is transported upward following the lower vortex and O_3 is transported downward following the upper vortex. Both rich NO and O_3 accelerate the O_3 depletion there and result in a large deviation from the chemical equilibrium. A large-eddy simulation (LES) study of Li et al. (2009) showed the field of the scalar mixing ratio budget similar to Fig. 3a and the larger vertical advection and turbulent diffusion terms in magnitude at the interface of two primary vortices than at the roof level in the $H/W = 2$ street canyon.

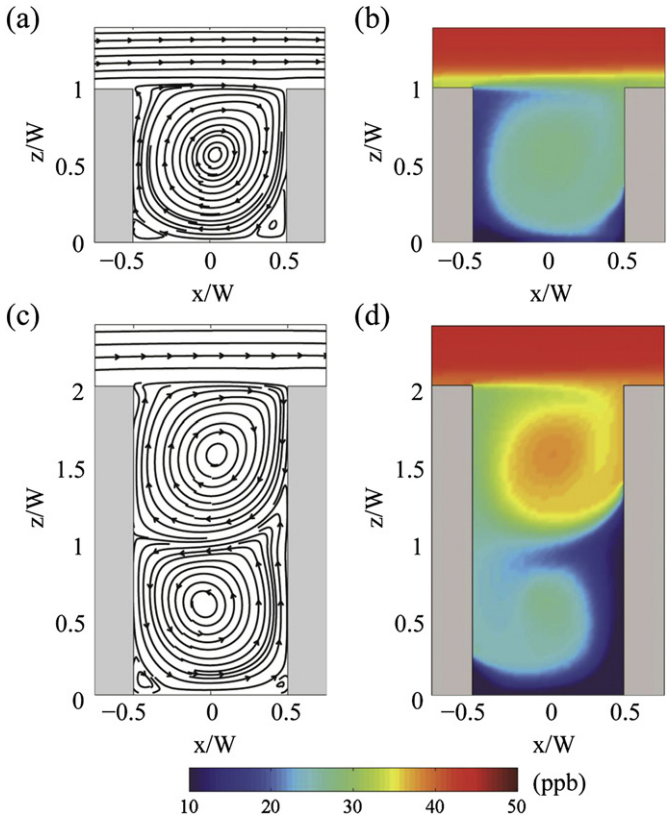

Fig. 2. (a, c) Streamline and (b, d) O_3 concentration fields in the street canyons with canyon aspect ratios of 1 (upper panels) and 2 (lower panels).

The concept of photochemical age introduced in this study is used to elucidate different O_3 chemical characteristics between the lower and upper regions of the street canyon. Fig. 4 shows scatter plots of the O_3 chemical production rate with the normalized photochemical ages of NO_x and VOC. The background NO_2/NO_x and TOL/XYL are 0.70 and 1.58, respectively. The average O_3 concentrations in t_{NO_x} and $t^{bg}_{NO_x}$ are set to be the same, and the average OH concentrations in t_{VOC} and t^{bg}_{VOC} are also set to be the same. In the scatter plots, a large proportion of grid points are concentrated near the line of a zero O_3 chemical production rate except for the two chemically active regions mentioned above. More precisely, the O_3 chemical production (up to 2 h^{-1}) is significant when $t_{NO_x}/t^{bg}_{NO_x}$ is larger than 0.55 (equivalent to $NO_2/NO_x = 0.51$) and t_{VOC}/t^{bg}_{VOC} is larger than 0.28 (equivalent to TOL/XYL = 1.17). It is interesting that the grid points plotted with t_{VOC}/t^{bg}_{VOC} in Fig. 4b are compactly distributed toward the left-hand side compared to the grid points plotted with $t_{NO_x}/t^{bg}_{NO_x}$ in Fig. 4a. In addition, Fig. 4b shows that t_{VOC}/t^{bg}_{VOC} at every grid point in the street canyon is smaller than 0.6, whereas the largest $t_{NO_x}/t^{bg}_{NO_x}$ is larger than 0.9 in Fig. 4a. These are

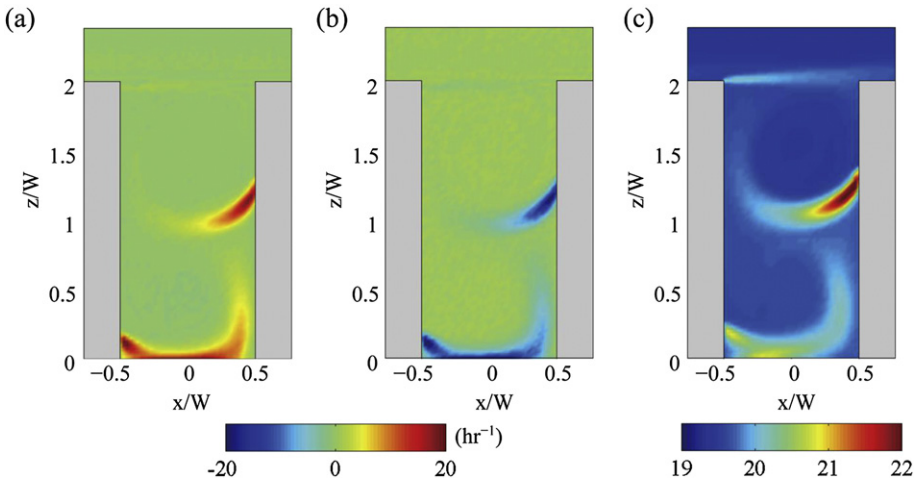

Fig. 3. Fields of O_3 (a) transport and (b) chemical production rates, which are divided by O_3 concentration at corresponding grid point, and (c) the field of photo-stationary state.

because the O_3 oxidation process is mostly completed in the street canyon, but the OH oxidation process continues even after an air mass escapes from the street canyon. In conclusion, $t_{NO_x}/t^{bg}_{NO_x}$ is well capable of capturing the photochemical evolution near the point of emission, while t_{VOC}/t^{bg}_{VOC} is well capable of capturing the photochemical evolution around the roof level.

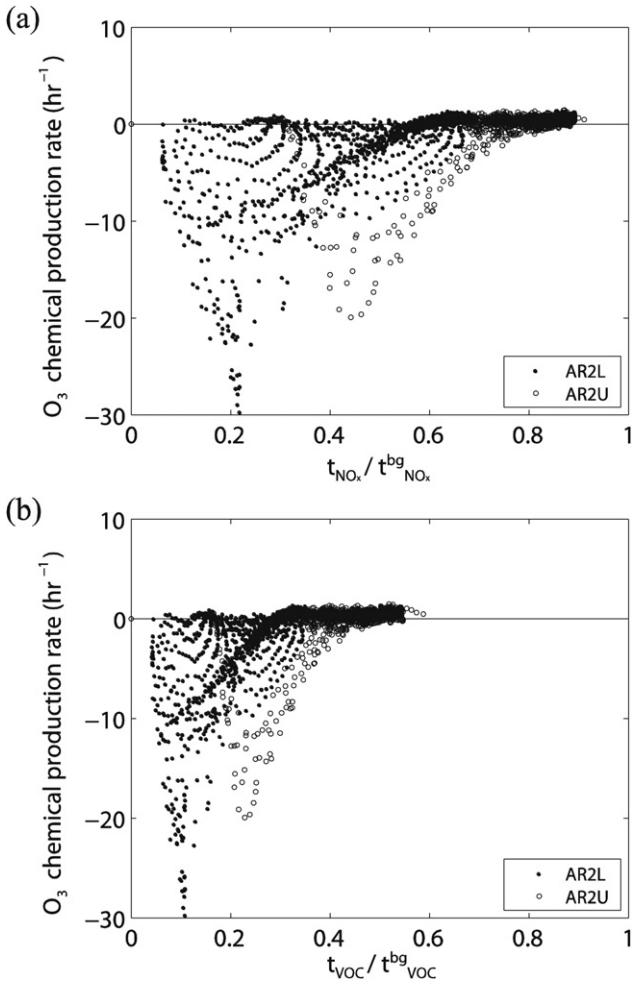

Fig. 4. Scatter plots of O_3 chemical production rate divided by O_3 concentration at corresponding grid point with (a) $t_{NO_x}/t^{bg}_{NO_x}$ and (b) t_{VOC}/t^{bg}_{VOC}. Closed and open circles indicate grid points in the lower and upper regions of the street canyon with a canyon aspect ratio of 2, respectively.

The normalized photochemical ages and their ratio are given in Table 2 using averaged concentrations of NO_2, NO_x, TOL, and XYL in the $H/W = 1$ street canyon (AR1), the $H/W = 2$ street canyon (AR2), and the lower (AR2L) and upper (AR2U) regions of the $H/W = 2$ street canyon. It is clear that the normalized photochemical ages are the smallest in AR2L. The normalized photochemical ages in AR2U are the largest, followed by those in AR1 and AR2. Compared to the normalized photochemical ages in AR1, those in AR2L indicate the characteristics close to the emission, whereas those in AR2U indicate the characteristics close to the background air. R_{PA} is larger than 1 in all cases. For example, in AR2U, $t_{NO_x}/t^{bg}_{NO_x}$ (0.76) is larger than t_{VOC}/t^{bg}_{VOC} (0.43), giving $R_{PA} = 1.77$. This means that the O_3 oxidation process is cumulatively faster than the OH oxidation process in the street canyons, which is in line with the finding from the comparison between Fig. 4a and b.

To quantitatively compare each contribution in AR1, AR2, AR2L, and AR2U, the area-averaged emission, transport, chemical production, and total (= emission + transport + chemical production) rates of NO, NO_2, O_3, XYL, FORM, and OH divided by their area-averaged concentrations are calculated (Fig. 5). NO and XYL that are emitted species at the street bottom are chemically reduced and transported upward in AR1 and AR2L. The large amounts of the transported NO and XYL remaining in AR2U are chemically reduced. The magnitudes of NO and XYL transport rates in AR2 are greatly reduced compared to those in AR1, which is consistent with the results of LES study (Cai et al., 2008) examining mean scalar fluxes at the roof level with different canyon aspect ratios. NO_2 and FORM that are emitted species at the street bottom are chemically produced and transported upward in AR1 and AR2L. The chemical production rates of NO_2 and FORM are even larger than their emission rates averaged over the regions. In AR2U, the chemical production of NO_2 and FORM is more pronounced than their transport. Overall, the total rates of NO_2 and FORM are positively

Table 2
$t_{NO_x}/t^{bg}_{NO_x}$, t_{VOC}/t^{bg}_{VOC}, and R_{PA} in the street canyons with canyon aspect ratios of 1 (AR1) and 2 (AR2) and the lower (AR2L) and upper (AR2U) regions of the street canyon with a canyon aspect ratio of 2.

	AR1	AR2L	AR2U	AR2
$t_{NO_x}/t^{bg}_{NO_x}$	0.56	0.40	0.76	0.50
t_{VOC}/t^{bg}_{VOC}	0.37	0.21	0.43	0.28
R_{PA}	1.51	1.90	1.77	1.79

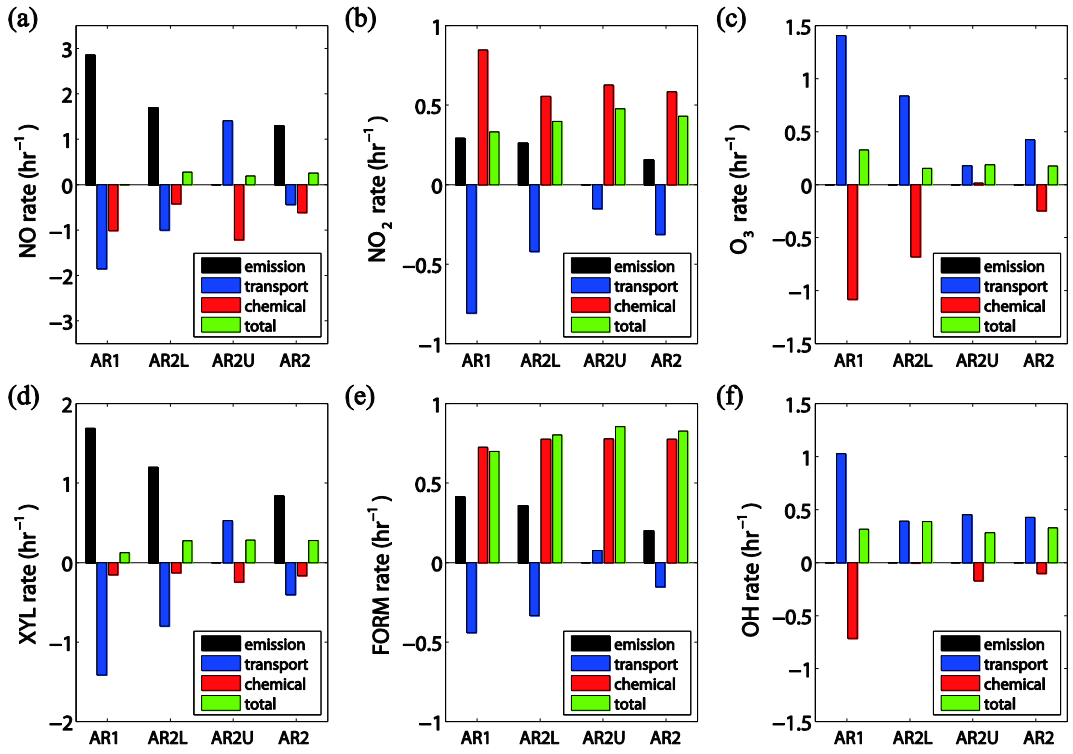

Fig. 5. Averaged emission, transport, chemical production, and total rates of (a) NO, (b) NO_2, (c) O_3, (d) XYL, (e) FORM, and (f) OH divided by their averaged concentrations in the street canyons with canyon aspect ratios of 1 (AR1) and 2 (AR2) and the lower (AR2L) and upper (AR2U) regions of the street canyon with a canyon aspect ratio of 2.

significant in all regions. O_3 is transported downward across the roof level in both AR1 and AR2. Whereas the transported O_3 is chemically reduced in AR1 and AR2L, O_3 is chemically produced in AR2U. This means that the NO titration of O_3 is less pronounced than the NO_2 photolysis in AR2U where the air is more aged than in AR1 and AR2L. OH is also transported downward across the roof level in both AR1 and AR2, while its chemical production rate is always negative.

4.2. Sensitivity experiments

In the control experiment, it was found that O_3 can be chemically produced in AR2U as well as transported downward across the roof level. The O_3 chemical production can be affected by conditions such as NO_x and VOC emission rates, photolysis rate, and ambient wind speed. Sensitivities to such conditions are examined for $H/W = 2$.

Fig. 6 shows area-averaged O_3 concentrations and area-averaged O_3 rates divided by the area-averaged O_3 concentrations at different NO_x and VOC emission rates. The O_3 concentration decreases with increasing NO_x emission rate but increases with increasing VOC emission rate in both AR2L and AR2U. For example, the O_3 concentration decreases by 9.0 ppb in AR2L and 10.0 ppb in AR2U when the NO_x emission rate increases from 2 to 4 ppb s^{-1}. On the other hand, the O_3 concentration increases by 5.5 ppb in AR2L and 5.0 ppb in AR2U when the VOC emission rate increases from 2 to 4 ppb s^{-1}. The changes in O_3 concentration are associated directly with the changes in O_3 chemical production rate and indirectly with those in O_3 transport rate. When the NO_x emission rate increases from 2 to 4 ppb s^{-1}, the O_3 chemical production rate decreases from -0.68 to -1.10 h^{-1} in AR2L and from 0.01 to -1.06 h^{-1} in AR2U. When the VOC emission rate increases from 2 to 4 ppb s^{-1}, the O_3 chemical production rate increases from -0.68 to -0.001 h^{-1} in AR2L and from 0.01 to 0.50 h^{-1} in AR2U. Although the changes in O_3 transport rate partially compensate for the changes in O_3 chemical production rate, the O_3 total rates generally follow the O_3 chemical production rates. A positive O_3 chemical production rate is exhibited when the NO_x emission rate is 1 ppb s^{-1} or the VOC emission rate is 6 ppb s^{-1} in AR2L but when the NO_x emission rate is 1 and 2 ppb s^{-1} or the VOC emission rate is 2, 4, and 6 ppb s^{-1} in AR2U. This result agrees with the result of Liu and Leung (2008) that high levels of O_3 would occur in street canyons when the ratio of VOC emission rate to NO_x emission rate is high.

Fig. 7 shows area-averaged O_3 concentrations and area-averaged O_3 rates divided by the area-averaged O_3 concentrations at different photolysis rates and ambient wind speeds. Here, a J-value coefficient of 0.2 denotes an 80% reduction in photolysis rate and a J-value coefficient of 1.0 denotes no reduction in photolysis rate. The O_3 concentration decreases with decreasing J-value coefficient. For example, the O_3 concentration decreases by 8.2 ppb in AR2L and 9.3 ppb in AR2U when the J-value coefficient decreases from 1.0 to 0.6. Reducing the photolysis rate causes the NO_2 photolysis to be less pronounced than the NO titration of O_3, resulting in a decreased O_3 chemical production rate followed by an increased O_3 transport rate and an increased O_3 total rate in the street canyon. When the J-value coefficient decreases from 1.0 to 0.6, the O_3 chemical production rate decreases from -0.68 to -1.28 h^{-1} in AR2L and from 0.01 to -1.05 h^{-1} in AR2U. A positive O_3 chemical production rate is not exhibited in AR2L but only exhibited in AR2U when the J-value coefficient is 1.0. It is interesting that the sensitivities of O_3 concentration and rate to the J-value coefficient are larger in AR2U than in AR2L. This may indicate more active photolysis processes in the more aged air than in the less aged air.

The sensitivity of O_3 concentration to the ambient wind speed is relatively small. The O_3 concentration slightly increases with increasing ambient wind speed in AR2L but varies very little in the ambient wind speed ranging from 4 to 7 m s^{-1} in AR2U. Increasing ambient wind speed enhances the mixing process in

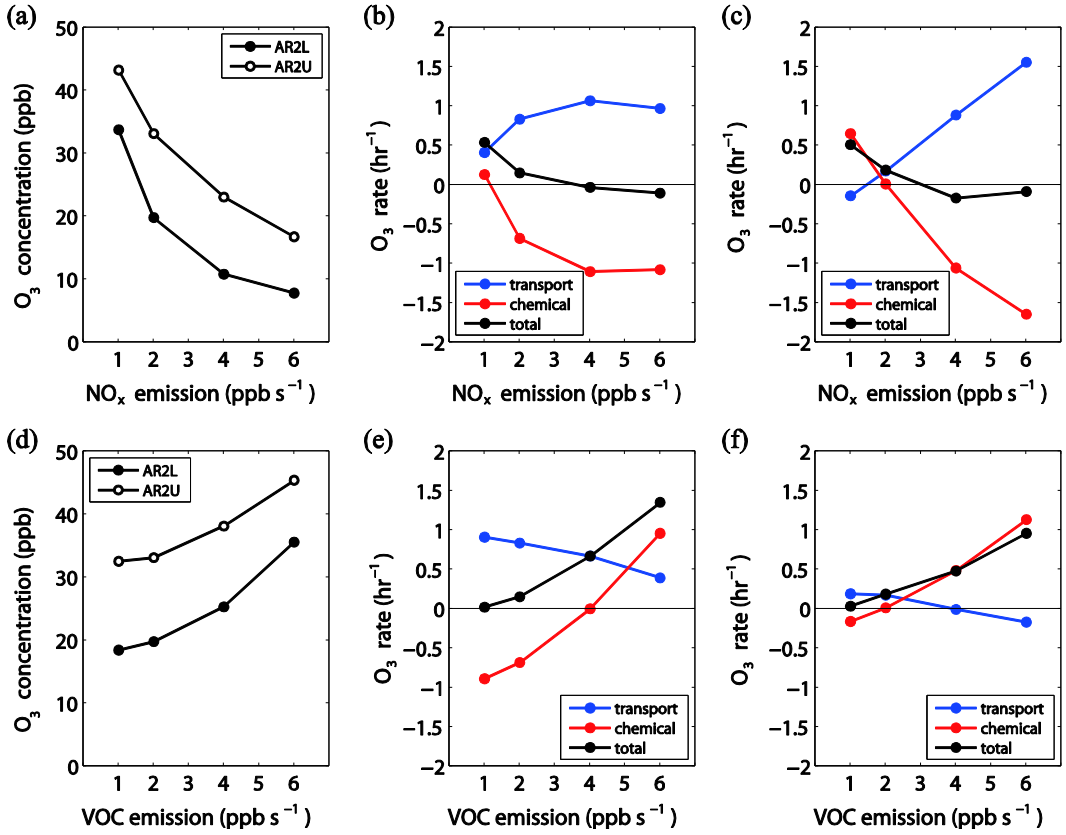

Fig. 6. Averaged O_3 concentrations (left panels) and averaged O_3 transport, chemical production, and total rates divided by the averaged O_3 concentrations in AR2L (middle panels) and AR2U (right panels) at different (a–c) NO_x and (d–f) VOC emission rates.

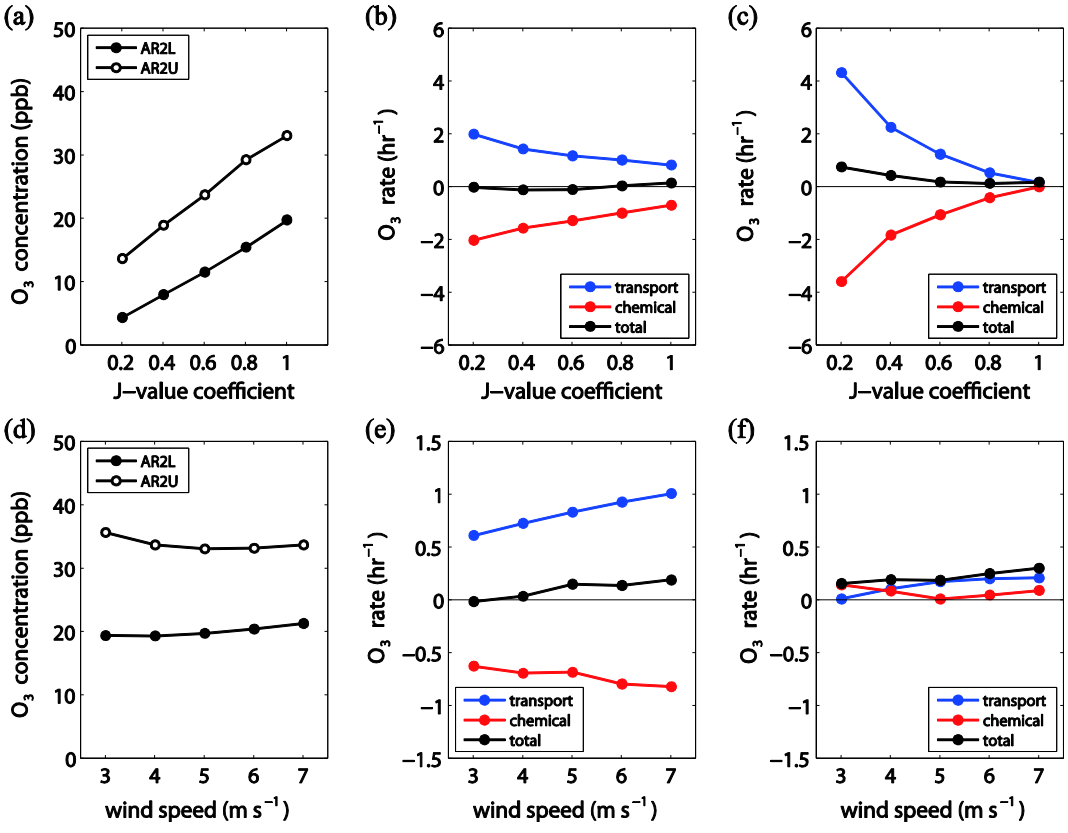

Fig. 7. Same as Fig. 6 but at different (a–c) photolysis rates and (d–f) ambient wind speeds.

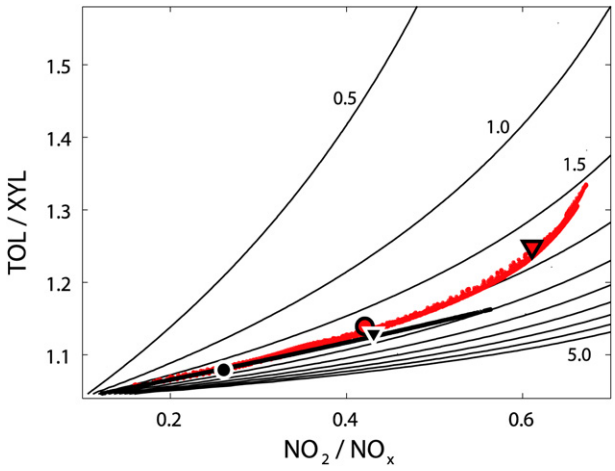

Fig. 8. A photochemical aging diagram plotting all grid points in the street canyon with a canyon aspect ratio of 2. R_{PA} is contoured with intervals of 0.5. Red and black dots indicate grid points in the simulation of chemistry-on and chemistry-off, respectively. Circles and inversed triangles are averaged points in the lower and upper regions of the street canyon, respectively.

the street canyon, resulting in strengthened upward transport of emitted pollutants and strengthened downward transport of O_3. When the ambient wind speed increases from 4 to 6 m s^{-1}, the O_3 transport rate increases from 0.73 to 0.93 h^{-1} in AR2L and from 0.11 to 0.20 h^{-1} in AR2U. A positive O_3 chemical production rate is not exhibited in AR2L but always exhibited in AR2U. The O_3 total rate generally follows the O_3 transport rate, while the contribution of O_3 transport to the O_3 concentration is not significant.

4.3. Photochemical aging diagram

A scatter diagram, referred to as the photochemical aging diagram, is plotted in Fig. 8 with NO_2/NO_x on the x-axis and TOL/XYL on the y-axis. R_{PA} is contoured on this diagram. The photochemical aging diagram captures the progress of the O_3 and OH oxidation processes. In estimating the relative importance between the oxidation processes at a certain grid point, a local increase in R_{PA} means that the O_3 oxidation process is relatively important, whereas a local decrease in R_{PA} means that the OH oxidation process is relatively important. In Fig. 8, black dots indicate the calculated concentration ratios at every grid point in the $H/W = 2$ street canyon when the chemical process is switched off during the model run. The constant slope of black dots between NO_2/NO_x and TOL/XYL reflects the mixing process only. On the other hand, red dots indicating the calculated concentration ratios at every grid point in the control experiment show larger concentration ratios and a decrease in R_{PA} especially for the aged air. The larger concentration ratios and the decrease in R_{PA} reflect the effect of chemical process. It is found from the decrease in R_{PA} that the OH oxidation process is relatively important in the upper region of the street canyon.

The photochemical aging diagram is used to analyze the results of the sensitivity experiments. Fig. 9a and b shows the progress of the O_3 and OH oxidation processes at different NO_x and VOC emission rates. R_{PA} decreases with increasing NO_x emission rate in both AR2L and AR2U, implying that the O_3 oxidation process is suppressed relative to the OH oxidation process as a result of the decrease in O_3 concentration due to the large amount of NO_x emission. On the other hand, R_{PA} increases with increasing VOC emission rate in both AR2L and AR2U, implying that the O_3 oxidation process is enhanced because of the increase in O_3 concentration. In Fig. 9c, R_{PA} increases with decreasing J-value coefficient.

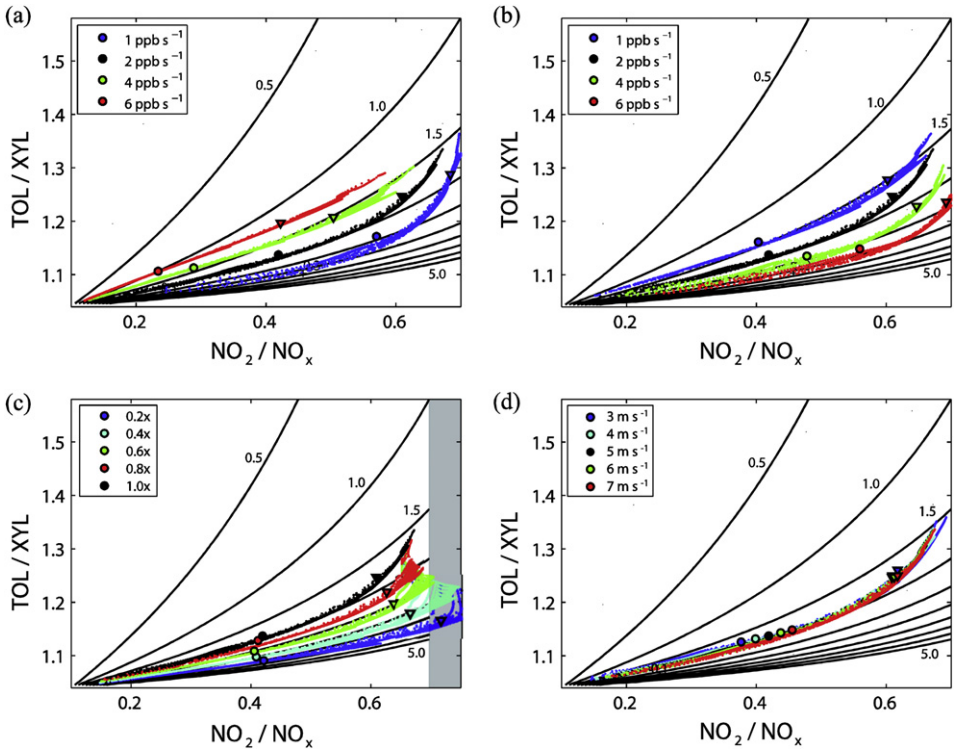

Fig. 9. Photochemical aging diagrams plotting all grid points in the street canyon with a canyon aspect ratio of 2 at different (a) NO_x and (b) VOC emission rates, (c) photolysis rates, and (d) ambient wind speeds. R_{PA} is contoured with intervals of 0.5. Circles and inversed triangles are averaged points in the lower and upper regions of the street canyon, respectively. Shaded area in c indicates NO_2/NO_x higher than the background value in the control experiment.

The OH oxidation process is more influential in the sensitivity to *J*-value coefficient in contrast to the sensitivities to NO_x and VOC emission rates. While the increase in O_3 concentration with increasing *J*-value coefficient is considerable (Fig. 7a), the OH concentrations in the case of a *J*-value coefficient of 1.0 are 8.9 and 7.8 times higher than those in the case of a *J*-value coefficient of 0.2 in AR2L and AR2U, respectively. This is the reason for the increase in R_{PA} with decreasing *J*-value coefficient. A distinctive point in Fig. 9c is the higher NO_2/NO_x (in the shaded area) near the roof level in the experiments with low *J*-value coefficients (i.e., 0.2, 0.4, and 0.6) than NO_2/NO_x in the background in the control experiment with a *J*-value coefficient of 1.0. The higher NO_2/NO_x is a result of the inefficient NO_2 photolysis. In Fig. 9d, R_{PA} shows little variation at different ambient wind speeds. It is clear that the air mass in the street canyon undergoes equivalent O_3 and OH oxidation processes. The increase in concentration ratios with increasing ambient wind speed is clear only in AR2L. As mentioned in Section 4.2, the enhanced mixing process accelerates the aging of the air mass as the ambient wind speed increases. However, the relative importance between O_3 and OH oxidation processes is not affected by the change in ambient wind speed.

5. Summary and conclusions

A CFD model coupled with the CBM–IV was used to investigate the dispersion and photochemical evolution of reactive pollutants in street canyons with canyon aspect ratios of 1 and 2. The photochemical ages of NO_x and VOC were derived and used to analyze the O_3 and OH oxidation processes. Various conditions were considered to examine the sensitivities of O_3 concentration and related transport and photochemical processes. The O_3 dispersion shows a distinct separation between the lower and upper regions of the $H/W = 2$ street canyon. It was found that O_3 is chemically produced in the upper region of the street canyon, whereas O_3 is chemically reduced in the lower region of the street canyon. A positive O_3 chemical production rate is favorable when the normalized photochemical ages of NO_x and VOC are larger than 0.55 and 0.28, respectively. Other reactive pollutants such as NO, NO_2, TOL, XYL, and OH also show differences in chemical characteristics between the lower and upper regions of the street canyon. The sensitivities of O_3 concentration and rate to NO_x and VOC emission rates, photolysis rate, and ambient wind speed were examined. The results show that the O_3 concentration increases with decreasing NO_x emission rate and increasing VOC emission rate and photolysis rate. The O_3 chemical production is favorable when the NO_x emission rate is low and the VOC emission rate and photolysis rate are high. The sensitivity of O_3 concentration to ambient wind speed appears within a few ppb. In the photochemical aging diagram, the relative importance between O_3 and OH oxidation processes was analyzed. The OH oxidation process becomes relatively important as the NO_x emission rate and photolysis rate increase and the VOC emission rate decreases. The sensitivity of the relative importance between O_3 and OH oxidation processes to ambient wind speed is negligible, but the sensitivities of NO_2/NO_x and TOL/XYL in the lower region of the street canyon are not negligible owing to the mixing process.

The photochemical ages of NO_x and VOC in this study are expressed to include both O_3 and OH oxidation processes that are important in street-canyon scale chemistry. By taking a concentration ratio of oxidant (i.e., O_3 or OH) in a normalized photochemical age, an uncertainty from estimating an average O_3 or OH concentration can be avoided. It was demonstrated that concentration ratios representing O_3 and OH oxidation processes are useful for characterizing an air mass in a street canyon. Furthermore, O_3 chemical production and its preferred conditions can be estimated using the photochemical age when the photochemical evolution of an air mass is examined not only in street-canyon scale chemistry but also in neighborhood scale chemistry. The photochemical evolution of an air mass from the point of emission in a neighborhood scale would be an interesting research subject.

Acknowledgments

The authors are grateful to two anonymous reviewers for providing valuable comments on this work. This work was supported by the National Research Foundation of Korea (NRF) grant funded by the Korea Ministry of Education, Science and Technology (MEST) (No. 2012-0005674) and also by the Brain Korea 21 Project (through the School of Earth and Environmental Sciences, Seoul National University).

References

Apel, E.C., Emmons, L.K., Karl, T., Flocke, F., Hills, A.J., Madronich, S., Lee-Taylor, J., Fried, A., Weibring, P., Walega, J., Richter, D., Tie, X., Mauldin, L., Campos, T., Weinheimer, A., Knapp, D., Sive, B., Kleinman, L., Springston, S., Zaveri, R., Ortega, J., Voss, P., Blake, D., Baker, A., Warneke, C., Welsh-Bon, D., de Gouw, J., Zheng, J., Zhang, R., Rudolph, J., Junkermann, W., Riemer, D.D., 2010. Chemical evolution of volatile organic compounds in the outflow of the Mexico City Metropolitan area. Atmospheric Chemistry and Physics 10, 2353–2376.

Baik, J.-J., Kim, J.-J., 1999. A numerical study of flow and pollutant dispersion characteristics in urban street canyons. Journal of Applied Meteorology 38, 1576–1589.

Baik, J.-J., Kim, J.-J., 2002. On the escape of pollutants from urban street canyons. Atmospheric Environment 36, 527–536.

Baik, J.-J., Kang, Y.-S., Kim, J.-J., 2007. Modeling reactive pollutant dispersion in an urban street canyon. Atmospheric Environment 41, 934–949.

Baker, J., Walker, H.L., Cai, X., 2004. A study of the dispersion and transport of reactive pollutants in and above street canyons—a large eddy simulation. Atmospheric Environment 38, 6883–6892.

Bossioli, E., Tombrou, M., Pilinis, C., 2002. Adapting the speciation of the VOCs emission inventory in the greater Athens area. Water, Air, and Soil Pollution: Focus 2, 141–153.

Cai, X.-M., Barlow, J.F., Belcher, S.E., 2008. Dispersion and transfer of passive scalars in and above street canyons—large-eddy simulations. Atmospheric Environment 42, 5885–5895.

Calvert, J.G., 1976. Hydrocarbon involvement in photochemical smog formation in Los Angeles atmosphere. Environmental Science and Technology 10, 256–262.

de Gouw, J.A., Middlebrook, A.M., Warneke, C., Goldan, P.D., Kuster, W.C., Roberts, J.M., Fehsenfeld, F.C., Worsnop, D.R., Canagaratna, M.R., Pszenny, A.A.P., Keene, W.C., Marchewka, M., Bertman, S.B., Bates, T.S., 2005. Budget of organic carbon in a polluted atmosphere: results from the New England air quality study in 2002. Journal of Geophysical Research 110 (D16305). http://dx.doi.org/10.1029/2004J005623.

Garmory, A., Kim, I.S., Britter, R.E., Mastorakos, E., 2009. Simulations of the dispersion of reactive pollutants in a street canyon, considering different chemical mechanisms and micromixing. Atmospheric Environment 43, 4670–4680.

Gery, M., Witten, G., Killus, J., Dodge, M., 1989. A photochemical kinetics mechanism for urban and regional scale computer modeling. Journal of Geophysical Research 94 (D10), 12925–12956.

Hertel, O., Berkowicz, R., Christensen, J., 1993. Test of two numerical schemes for use in atmospheric transport-chemistry models. Atmospheric Environment 27A, 2591–2611.

Kim, M.J., Park, R.J., Kim, J.-J., 2012. Urban air quality modeling with full O_3–NO_x–VOC chemistry: implications for O_3 and PM air quality in a street canyon. Atmospheric Environment 47, 330–340.

Kleinman, L.I., Daum, P.H., Lee, Y.-N., Nummermacker, L.J., Springston, S.R., Weinstein-Lloyd, J., Hyde, P., Doskey, P., Rudolph, J., Fast, J., Berkowitz, C., 2003. Photochemical age determinations in the Phoenix metropolitan area. Journal of Geophysical Research 108 (D3). http://dx.doi.org/10.1029/2002JD002621.

Kwak, K.-H., Baik, J.-J., 2012. A CFD modeling study of the impacts of NO_x and VOC emissions on reactive pollutant dispersion in and above a street canyon. Atmospheric Environment 46, 71–80.

Li, X.-X., Liu, C.-H., Leung, D.Y.C., 2009. Numerical investigation of pollutant transport characteristics inside deep urban street canyons. Atmospheric Environment 43, 2410–2418.

Liu, C.-H., Leung, D.Y.C., 2008. Numerical study on the ozone formation inside street canyons using a chemistry box model. Journal of Environmental Sciences 20, 832–837.

McKeen, S.A., Liu, S.C., Hsie, E.-Y., Lin, X., Bradshaw, J.D., Smyth, S., Gregory, G.L., Blake, D.R., 1996. Hydrocarbon ratios during PEM-WEST A: a model perspective. Journal of Geophysical Research 101 (D1), 2087–2109.

Nelson, P.F., Quigley, S.M., 1983. The m, p-xylenes: ethylbenzene ratio. A technique for estimating hydrocarbon age in ambient atmospheres. Atmospheric Environment 17, 659–662.

Parrish, D.D., Stohl, A., Forester, C., Atlas, E.L., Blake, D.R., Goldan, P.D., Kuster, W.C., de Gouw, J.A., 2007. Effects of mixing on evolution of hydrocarbon ratios in the troposphere. Journal of Geophysical Research 112 (D10S34). http://dx.doi.org/10.1029/2006JD007583.

Roberts, J.M., Fehsenfeld, F.C., Liu, S.C., Bollinger, M.J., Hahn, C., Albritton, D.L., Sievers, R.E., 1984. Measurements of aromatic hydrocarbon ratios and NO_x concentrations in the rural troposphere: observation of air mass photochemical aging and NO_x removal. Atmospheric Environment 18, 2421–2432.

Rudolph, J., Johnen, F.J., 1990. Measurements of light atmospheric hydrocarbons over the Atlantic in regions of low biological activity. Journal of Geophysical Research 95 (D12), 20583–20591.

Wang, Y.J., DenBleyker, A., McDonald-Buller, E., Allen, D., Zhang, K.M., 2011. Modeling the chemical evolution of nitrogen oxides near roadways. Atmospheric Environment 45, 43–52.